by H_x and H_z being singular[1] at the vane edges, making the surface currents and hence the power loss at these locations quite large. Of course, in the practical cavity the conductivity is not perfect and the fields would not be singular. Also, better convergence is obtained with thicker vanes, for which the fields are better behaved. Results of this Q calculation are presented in graphical form in Figs. 9 and 10. It is estimated that the calculated Q results are better than ± 10 percent accurate for $t/a < 0.1$ and better than ± 5 percent for $t/a > 0.1$. A useful check on the Q calculation is possible when $t/a = 1.0$. In this case the cavity is no longer open ended and is a simple closed rectangular cavity for which the Q is easily calculated [6] and found to agree with the results from this analysis. Note that the Q of the rectangular open-ended cavity is lower than the Q of a closed cavity of the same resonant frequency. The Q of the two constructed cavities was measured and found to be significantly lower (~ 60 percent) than the theoretical Q. This difference, which is quite common, is accounted for by the coupling hole size (0.2 in) and the surface finish, which was not polished or even very smooth.

VI. Conclusion

A field analysis of rectangular open-ended cavities has been presented. The resonant frequency and Q have been derived and presented in graphical form. Expressions for the fields inside the cavity were written and plotted in three dimensions. Good accuracies were obtained in the resonant frequency calculation; however, the Q calculation was not as well behaved due to the power loss becoming large at the vane edge. Comparisons of theoretical and experimental results for two constructed cavities were given.

Topics for further work include improvement of the Q calculation and quantifying the effect of a coupling hole on the cavity frequency and Q. Variations in the cavity design such as unsymmetrical terminations or more than one vane in each termination region could also be investigated.

[1] As a reviewer has pointed out, only H_z is strictly singular while H_x has a step change equal to J_s at the discontinuity.

References

[1] R. O. Gilmer and D. C. Thorn, "Some design criteria for open-ended microwave cavities," Univ. New Mexico, Albuquerque, Tech. Rept. EE-65, June 1962.

[2] N. C. Wenger, "Resonant frequency of open-ended cylindrical cavity," *IEEE Trans. Microwave Theory Tech.*, vol. MTT-15, pp. 334–340, June 1967.

[3] R. E. Collin, *Field Theory of Guided Waves.* New York: McGraw-Hill, 1960, pp. 447–449.

[4] R. Mittra and S. Lee, *Analytical Techniques in the Theory of Guided Waves.* New York: Macmillan, 1971, pp. 30–45.

[5] A. Wexler, "Solution of waveguide discontinuities by modal analysis," *IEEE Trans. Microwave Theory Tech.*, vol. MTT-15, pp. 508–517, Sept. 1967.

[6] R. E. Collin, *Foundations for Microwave Engineering.* New York: McGraw-Hill, 1966, pp. 324–325.

[7] D. M. Pozar, "Field analysis of an open-ended rectangular microwave cavity," M.S. thesis, University of Akron, Akron, OH, June 1976.

[8] R. Mittra, T. Itoh, and T. S. Li, "Analytical and numerical studies of the relative convergence phenomenon arising in the solution of an integral equation by the moment method," *IEEE Trans. Microwave Theory Tech.*, vol. MTT-20, pp. 96–104, Feb. 1972.

Ferrite Planar Circuits in Microwave Integrated Circuits

TANROKU MIYOSHI, MEMBER, IEEE, S. YAMAGUCHI, AND SHINJI GOTO

Abstract—**The ferrite planar circuit to be discussed in this paper is a general planar circuit using ferrite substrates magnetized perpendicular to the ground conductors. The main subject of this paper is the analysis of an arbitrarily shaped triplate ferrite planar circuit. In particular, the circuit parameters of the equivalent multiport are determined. To analyze ferrite planar circuits in general, two approaches are possible. One approach is based upon a contour-integral solution of the wave equation. In the other approach the fields in the circuit are expanded in terms of orthonormal eigenfunctions. Examples of the application of such analyses are described.**

Manuscript received September 7, 1976; revised December 17, 1976.
The authors are with the Department of Electronic Engineering, Kobe University, Kobe, Japan.

I. Introduction

THE planar circuit is defined as an electrical circuit whose thickness in one direction is much less than one wavelength and whose dimensions in the orthogonal directions are comparable to the wavelength. The concept of the planar circuit was proposed by Okoshi in 1969 [1]. Since then, its analysis [2]–[5] and synthesis [6], [7] have been investigated for many circuits using isotropic material for the spacer.

This paper will present the general treatment of a planar circuit using ferrite material for the spacer. In particular, an arbitrarily shaped ferrite planar circuit is discussed. The

ferrite is magnetized in the direction perpendicular to the ground plane.

Stripline circulators [8] often used in the microwave integrated circuits and edge-guided mode devices [9], [10] are considered ferrite planar circuits. They are, strictly speaking, two-dimensional circuits because they require essentially a disk resonator, wide striplines, and tapered sections.

The main subject of this paper is the analysis of an arbitrarily shaped, triplate ferrite planar circuit. In particular, the circuit parameters of the equivalent multiport are determined. To analyze ferrite planar circuits in general, two approaches are possible. One approach is based upon a contour-integral solution of the wave equation. In the other approach the fields in the circuit are expanded in terms of orthonormal eigenfunctions. Examples of such analyses are also described.

II. Basic Equation

A ferrite planar circuit consists of an arbitrarily shaped thin center conductor sandwiched by two ferrite substrates with magnetic field perpendicular to the conducting plate. It is assumed to be excited symmetrically with respect to the upper and lower ground conductors. There are several coupling ports as shown in Fig. 1 and the remainder of the periphery is assumed to be open circuited. The xy coordinates and z axis, respectively, are set parallel and perpendicular to the conductors. The bias magnetization is in the z direction. The thickness of the planar circuit is $2d$.

When the spacing d is much smaller than the wavelength and ferrite spacers are homogeneous and linear, only the field components E_z, H_x, and H_y with no variation along the z axis are considered. It is deduced directly from Maxwell's equation that the following equation governs the electromagnetic fields in the ferrite planar circuit:

$$(\nabla_T^2 + \omega^2\varepsilon\mu_{\text{eff}})V = 0 \tag{1}$$

where

$$\nabla_T^2 = \frac{\partial^2}{\partial x^2} + \frac{\partial^2}{\partial y^2} \qquad \mu_{\text{eff}} = \frac{\mu^2 - \kappa^2}{\mu}.$$

Here V given by $E_z \times d$ denotes the RF voltage of the center conductor with respect to the ground conductors. The effective permeability μ_{eff} is given by μ and κ which are the diagonal and off-diagnonal coefficients of permeability tensor for magnetization in the z direction. The sign of μ_{eff} will depend upon the frequency and the internal magnetic field.

At a coupling port, the following boundary condition given by the differential equation must apply:

$$j\frac{\kappa}{\mu}\frac{\partial V}{\partial t} + \frac{\partial V}{\partial n} = -j\omega\mu_{\text{eff}}\, di_n \tag{2}$$

where i_n is the surface current density normal to the periphery and ∂n and ∂t, respectively, are the derivative normal to the periphery and the tangential derivative around the periphery.

Almost at the periphery where the coupling ports are absent, the current flow normal to the periphery is assumed to be zero, that is, $i_n = 0$. Actually, however, the fringing magnetic fields are always present. A simple correction for this effect is to enlarge the periphery outwards by an amount of $0.447d \times K (K = 0.4)$ in advance of the analysis. The coefficient K was determined by comparing the measured resonant frequencies for the various ferrite planar resonators with the theoretical ones, which were calculated by the Rayleigh–Ritz variational method assuming that the circuits were lossless. This will be explained later in Section IV-C.

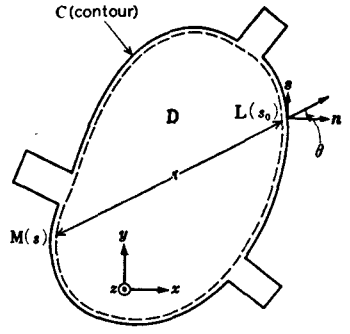

Fig. 1. Center conductor of a ferrite planar circuit and symbols used in the integral equation.

III. Analysis Based Upon a Contour-Integral Equation

A. Integral Equation

If we introduce Green's function G for (1), the RF voltage V_p at a point P in the circuit is given by a line integral

$$V_P = \oint_c \left\{ -j\omega\mu_{\text{eff}}\, di_n G + V\left(j\frac{\kappa}{\mu}\frac{\partial G}{\partial t} - \frac{\partial G}{\partial n}\right)\right\} dt. \tag{3}^1$$

If we now use the free-space Green's function for G in (3), then we must select different types of Green's functions according to the sign of μ_{eff}.

When $\mu_{\text{eff}} > 0$, $G = H_0^{(2)}(kr)/4j$ should be used as Green's function, where $H_0^{(2)}$ is the zeroth-order Hankel function of second kind and $k = \omega\sqrt{\varepsilon\mu_{\text{eff}}}$. Then from (3), the RF voltage at a point upon the periphery is found to satisfy the following equation:

$$V_M = \frac{1}{2j}\oint_c \left\{ j\omega\mu_{\text{eff}}\, dH_0^{(2)}(kr)(-i_n) + k\left(\cos\theta - j\frac{\kappa}{\mu}\sin\theta\right) H_1^{(2)}(kr)V_L\right\} dt. \tag{4}$$

In this equation $H_1^{(2)}$ is the first-order Hankel function of second kind. The variable r denotes distance between points M and L represented by s and s_0, respectively, and θ denotes

[1] $V_p = \oint_c \left\{G\frac{\partial V}{\partial n} - V\frac{\partial G}{\partial n}\right\} dt$
$= \oint_c \left\{G\left(\frac{\partial V}{\partial n} + j\frac{\kappa}{\mu}\frac{\partial V}{\partial t}\right) - j\frac{\kappa}{\mu}\frac{\partial V}{\partial t}G - V\frac{\partial G}{\partial n}\right\} dt.$
This relation and the relations (2) and $\oint_c G(\partial V/\partial t)\, dt = -\oint_c V(\partial G/\partial t)\, dt$ give (3).

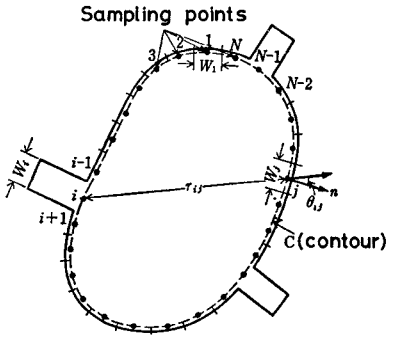

Fig. 2. Symbols used in the computer analysis.

the angle made by the straight line from point M to point L and the normal at point L as shown in Fig. 1. If the current density i_n injected upon the periphery is known, (4) becomes a Fredholm integral equation of the second kind in terms of the RF voltage.

B. Computational Formulation

For a numerical calculation, we divide the periphery into N incremental sections and set N sampling points defined at the center of each section as shown in Fig. 2. When we assume that the magnetic and electric field intensities are uniform across each section, the above integral equation results in a matrix equation:

$$\sum_{j=1}^{N} u_{ij}V_j = \sum_{j=1}^{N} h_{ij}I_j, \qquad i = 1,2,\cdots,N \tag{5}$$

where

$$u_{ij} = \delta_{ij} - \frac{k}{2j}\int_{W_j}\left\{\cos\theta - j\frac{\kappa}{\mu}\sin\theta\right\} H_1^{(2)}(kr)\,dt_j$$

$$h_{ij} = \begin{cases} \dfrac{\omega\mu_{\text{eff}}\,d}{4W_j}\displaystyle\int_{W_j} H_0^{(2)}(kr)\,dt_j, & i = j \\ \dfrac{\omega\mu_{\text{eff}}\,d}{4}\left\{1 - \dfrac{2}{\pi}\left(\log\dfrac{kW_i}{4} - 1 + \gamma\right)\right\}, & i = j \end{cases} \tag{6}$$

where $\gamma = 0.5772\cdots$: Euler's constant and $I_j = -2i_nW_j$ represents the total current flowing into the jth port. The formulas u_{ij} and h_{ij} in (6) have been derived assuming that the jth section is straight. From the above relations, the impedance matrix of the equivalent N-port is given by

$$Z = U^{-1}H \tag{7}$$

where U^{-1} denotes the inverse matrix to U. Then one element of the impedance matrix is given by

$$Z_{ij} = \frac{1}{\det U}\begin{vmatrix} u_{11} & \cdots & h_{1j} & \cdots & u_{1N} \\ \vdots & & \vdots & & \vdots \\ u_{N1} & \cdots & h_{Nj} & \cdots & u_{NN} \end{vmatrix}. \tag{8}$$

When the circuit has no coupling port, that is, $I_j = 0$, from the nontrivial condition of (5), we have

$$\det U = 0. \tag{9}$$

This equation gives the resonant frequency of the circuit.

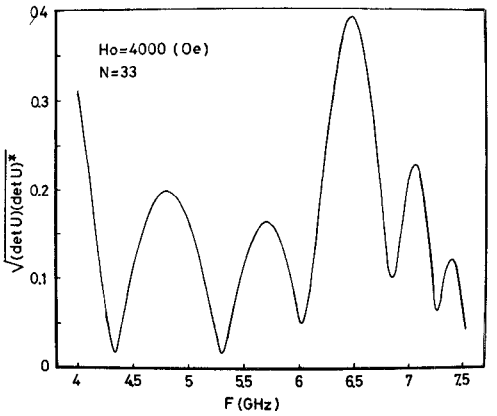

Fig. 3. The variation of $|\det U|$ as a function of frequency of a disk-shaped circuit at $H_0 = 4000$ Oe for $N = 33$.

When $\mu_{\text{eff}} < 0$, $G = \{K_0(hr) + j\pi I_0(hr)\}/2\pi$ is applicable, where $h = \omega\sqrt{\varepsilon|\mu_{\text{eff}}|}$ and I_0 and K_0 are the zeroth-order modified Bessel functions of the first and second kind, respectively. In this case the elements of matrices U and H in (7) are given by

$$u_{ij} = \delta_{ij} - \frac{h}{\pi}\int_{W_j}\left(\cos\theta - j\frac{\kappa}{\mu}\sin\theta\right)(K_1 - j\pi I_1)\,dt$$

$$h_{ij} = \begin{cases} \dfrac{j\omega\mu_{\text{eff}}\,d}{2\pi}\dfrac{1}{W_j}\displaystyle\int_{W_j}(K_0 + j\pi I_0)\,dt, & i \neq j \\ -\dfrac{j\omega\mu_{\text{eff}}\,d}{2\pi}\left\{\left(\log\dfrac{hW_i}{4} + \gamma - 1\right) - j\pi\right\}, & i = j. \end{cases} \tag{10}$$

C. Examples of Analysis

In all of the following examples, the ferrimagnetic material is assumed to be lossless with the saturation magnetization $4\pi M_s = 1300$ G, the dielectric constant $\varepsilon = 15.6$, and the thickness $d = 2$ mm.

As an example of the computer analysis described so far, the resonant frequencies of a disk-shaped circuit were computed first to check the computation accuracy. Since $\det U = 0$ in (9) is never realized for real frequency due to the computation error, we define the frequency which gives the minimum of $|\det U|$ as the eigenvalue. The variation of $|\det U|$ is shown as a function of frequency F (gigahertz) in Fig. 3 for $N = 33$ at $H_0 = 3300$ Oe, which shows the first ($F = 4.35$), the second ($F = 5.31$), the third ($F = 6.05$), the fourth ($F = 6.85$), and the fifth ($F = 7.26$) minima. By comparing these calculated eigenvalues with the theoretical ones, which should be given by the roots of

$$J_n'(ka) - \frac{\kappa}{\mu}\frac{nJ_n(ka)}{ka} = 0, \qquad n = 0, \pm1, \pm2\cdots$$

$$I_n'(ha) - \frac{\kappa}{\mu}\frac{nI_n(ha)}{ha} = 0, \qquad n = 1, 2\cdots$$

we found that the computation error was within 2.0 percent for the sampling number 33.

Next, the characteristics of the Y-junction stripline circulator were computed as shown in Fig. 4. Here the

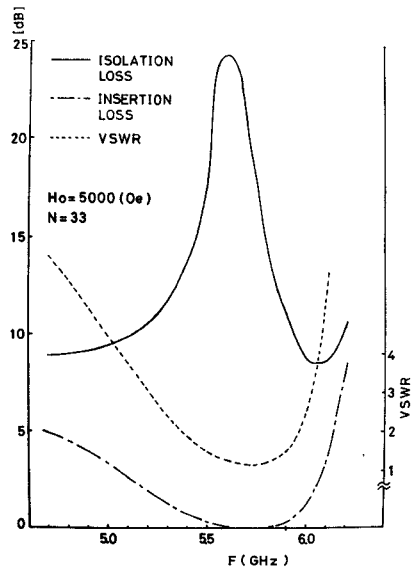

Fig. 4. Computed performance of a stripline Y-junction circulator coupled by the striplines of 50 Ω.

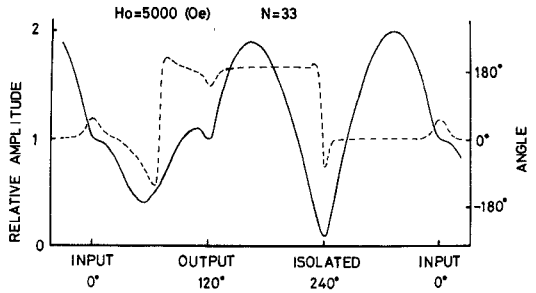

Fig. 5. Computed RF voltage distribution, amplitude (solid curve) and phase (broken curve), along the periphery of a Y-junction stripline circulator at the center frequency for $N = 33$.

internal magnetic field is 3700 Oe, $N = 33$, and 50-Ω striplines are coupled to the circulator. The circulator performance in Fig. 4 is obtained above the ferrimagnetic resonance point of circulation, which is about 5.7 GHz in this case. On the other hand, the resonant frequencies of $+1$ and -1 modes, respectively, are 5.5 and 4.9 GHz, which means that the center frequency is not midway between $+1$ and -1 mode resonant frequencies but exterior to the region. This is believed to be due to operating at a frequency far from the degeneracy of the ± 1 modes, i.e., at a greater separation of the modes, and the strong influence of higher order modes. Fig. 5 shows the RF voltage distribution along the periphery of a Y-junction stripline circulator at the center frequency for $N = 33$. The solid and broken curves show the relative amplitude and phase of the RF voltage along the periphery, respectively. The distribution of the amplitude is not sinusoidal, as might be expected, but exhibits a shallower minimum between the input and output ports and a distortion in the vicinity of ports. This is due to the influence of higher order modes as mentioned previously, which results from the strong coupling to the stripline ports.

IV. Analysis Based Upon an Eigenfunction Expansion

A. Formulation of Circuit Parameters

Now we introduce the Green's function which satisfies the following boundary condition along the contour C in (3):

$$j\frac{\kappa}{\mu}\frac{\partial G}{\partial t} - \frac{\partial G}{\partial n} = 0. \tag{11}$$

The RF voltage at a point in the circuit is given by

$$V = j\omega\mu_{\text{eff}}\, d \oint_c G(-i_n)\, dt. \tag{12}$$

Furthermore, we expand the Green's function in terms of the complex eigenfunctions ϕ_a which derive from the eigenvalue problem defined by

$$\begin{aligned} &(\nabla_T{}^2 + \omega_a{}^2\varepsilon\mu_{\text{eff}})\phi_a = 0, \qquad (\text{in } D) \\ &j\frac{\kappa}{\mu}\frac{\partial\phi_a}{\partial t} - \frac{\partial\phi_a}{\partial n} = 0, \qquad (\text{on } C) \\ &\iint_D \varepsilon\phi_a\phi_b^*\, dS = \delta_{ab} \end{aligned} \tag{13}$$

where the asterisk means a complex conjugate of ϕ_b. Then we can represent the RF voltage in the circuit, using eigenfunctions, by

$$V = j\omega\, d \oint_c \sum_{a=0}^{\infty} \frac{\phi_a\phi_a^*}{\omega_a{}^2 - \omega^2}(-i_n)\, dt. \tag{14}$$

Next, to calculate the circuit parameters of the equivalent multiport, we define approximately the RF voltage on a port and the total current flowing into a port, respectively, as

$$V_i = \frac{1}{W_i}\int_{W_i} V(t_i)\, dt_i \qquad I_j = \int_{W_j} \{-2i_n(t_j)\}\, dt_j. \tag{15}$$

Substituting (15) into (14), we have

$$V_i = \sum_{j=1}^{l}\left(\sum_{a=0}^{\infty}\frac{j\omega\, d}{2W_iW_j}\int_{W_i}\int_{W_j}\frac{\phi_a^*(t_j)\phi_a(t_i)}{\omega_a{}^2 - \omega^2}\, dt_i\, dt_j\right) I_j \tag{16}$$

where l is the number of ports coupling to the planar circuit. Thus one element of the impedance matrix of the equivalent multiport becomes

$$Z_{ij} = \sum_{a=0}^{\infty}\frac{j\omega\, d}{2W_iW_j}\int_{W_i}\int_{W_j}\frac{\phi_a^*(t_i)\phi_a(t_j)}{\omega_a{}^2 - \omega^2}\, dt_i\, dt_j. \tag{17}$$

It is clear from the above equation that the impedance matrix is not symmetric, i.e., $Z_{ij} \neq Z_{ji}$, because ϕ_a are generally complex eigenfunctions, but $Z_{ij} = -Z_{ji}{}^*$, which corresponds to the lossless condition of the circuit. To obtain the performance of a ferrite planar circuit by means of (17), we must solve the eigenvalue problem defined by (13) repeatedly at different frequencies for a given circuit and a given bias magnetic field. This is due to the fact that μ_{eff} contained in the problem is a function of the operation frequency even if the bias magnetic field is given.

B. Computational Formulation

To solve the eigenvalue problem in (13), in general, the Rayleigh–Ritz variational method, using a polynomial approximation, will be employed.

Since (13) is found to be the Euler equation of the functional I,

$$I = \iint_D (|\nabla_T \phi|^2 - \omega^2 \varepsilon \mu_{\text{eff}} |\phi|^2)\, dS + j \frac{\kappa}{\mu} \oint_c \phi^* \frac{\partial \phi}{\partial t}\, dt. \tag{18}$$

Instead of solving (13), we attempt to find the approximate complex functions which minimize the functional I.

Let the function ϕ be replaced by

$$\phi = \sum_{i=1}^{M} c_i f_i \tag{19}$$

where the c_i denote the complex expansion coefficients to be determined and the f_i are the real basis functions. The stationary points of I can be selected by evaluating the M equations $\partial I/\partial c_i^* = 0$. This immediately gives the matrix eigenvalue problem

$$(A - \omega^2 \varepsilon \mu_{\text{eff}} B)c = 0 \tag{20}$$

where

$$A_{ij} = \iint_D \nabla f_i \cdot \nabla f_j\, dS + j \frac{\kappa}{\mu} \oint_c f_i \frac{\partial f_j}{\partial t}\, dt,$$

$$B_{ij} = \iint_D f_i f_j\, dS.$$

Here, the values of μ, κ, and μ_{eff} are constant if both the bias magnetic field and the frequency are given. Thus the eigenvalue problem given in (13) has been approximated by the algebraic eigenvalue problem contained in (20). In (20), noting that the A matrix is Hermitian and that the B matrix is symmetric and positive definite, the eigenvalue ω_a^2 is found to be real. The problem given in (20) will be solved easily by a library program when (20) is rewritten in the usual form of the eigenvalue problem of a Hermitian matrix. To normalize the approximating eigenfunctions having arbitrary amplitude, the coefficients calculated should be multiplied by

$$\left(\varepsilon \sum_{i=1}^{M} \sum_{j=1}^{M} c_i^* c_j B_{ij} \right)^{-1/2}$$

When the ferrite planar circuit has no coupling ports, i.e., in the case of a resonator, from the nontrivial condition of (20), we also have

$$\det (A - \omega^2 \varepsilon \mu_{\text{eff}} B) = 0. \tag{21}$$

However, in this case the angular frequency ω contained implicitly in μ, κ, and μ_{eff} is unknown. The resonant frequencies of the circuit are given by the roots of (21).

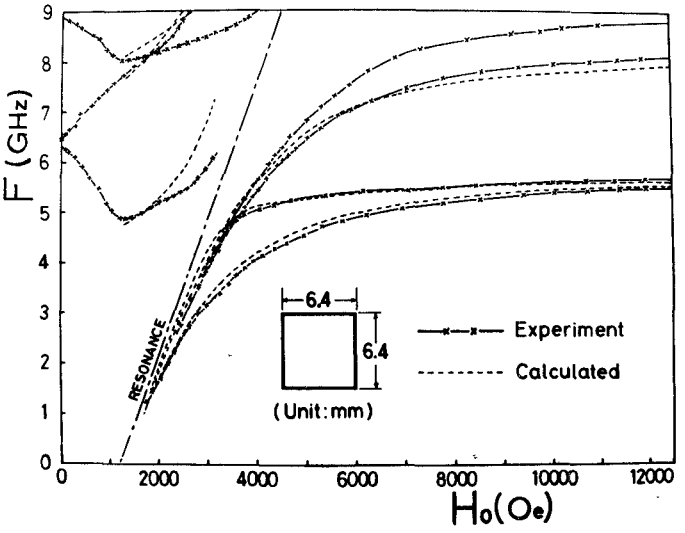

Fig. 6. Magnetic tuning characteristics of a square resonator. The broken curves were calculated taking fringing fields into account.

C. Results

In all of the following examples, a polynomial of order 5 will be used to approximate the eigenfunctions, which gives a matrix size of order 21.

First, the characteristics of ferrite planar resonators, of which nothing has been reported so far except a disk-shaped circuit [11], were studied. Fig. 6 shows the magnetic tuning characteristics of a square resonator with a side 6.4 mm long. The broken curves were calculated taking the effects of fringing fields into account as mentioned in Section II, assuming that the circuits are lossless. The measured resonant frequencies shown in solid curves are found to be in good agreement with the calculated values, especially above the ferrimagnetic resonance. This is probably because the influence of the magnetic loss is smaller in this region. In the experiment, the square ferrimagnetic substrates (25 × 25 mm^2) with a saturation magnetization of $4\pi Ms = 1300$ G, linewidth $\Delta H = 68$ Oe, a dielectric constant of $\varepsilon = 15.6$, and thickness $d = 2$ mm were used for the spacing material.

Fig. 7 shows the computed instantaneous distribution of the RF voltage in the square resonator for the fundamental mode. Equiamplitude (upper) and phase (lower) lines are shown for (a) $\mu_{\text{eff}} > 0$ at $H_0 = 1300$ Oe, and (b) $\mu_{\text{eff}} < 0$ at $H_0 = 2300$ Oe. The fields are found to rotate clockwise as in a disk resonator. It is also found that the fields are somewhat concentrated along the periphery when $\mu_{\text{eff}} < 0$.

In the case of a triangular resonator with a side 10 mm long, the magnetic tuning characteristics and the instantaneous RF voltage distribution for the fundamental mode are shown in Figs. 8 and 9, respectively. It is found from the figures that almost the same resonant characteristics as obtained for a square resonator result. It generally follows that when $\mu_{\text{eff}} > 0$, the modes rotating both clockwise and counterclockwise are the ones resonating in ferrite planar resonators. On the other hand, when $\mu_{\text{eff}} < 0$, only the mode rotating clockwise can exist, and, furthermore, the fields in resonators are concentrated along the periphery.

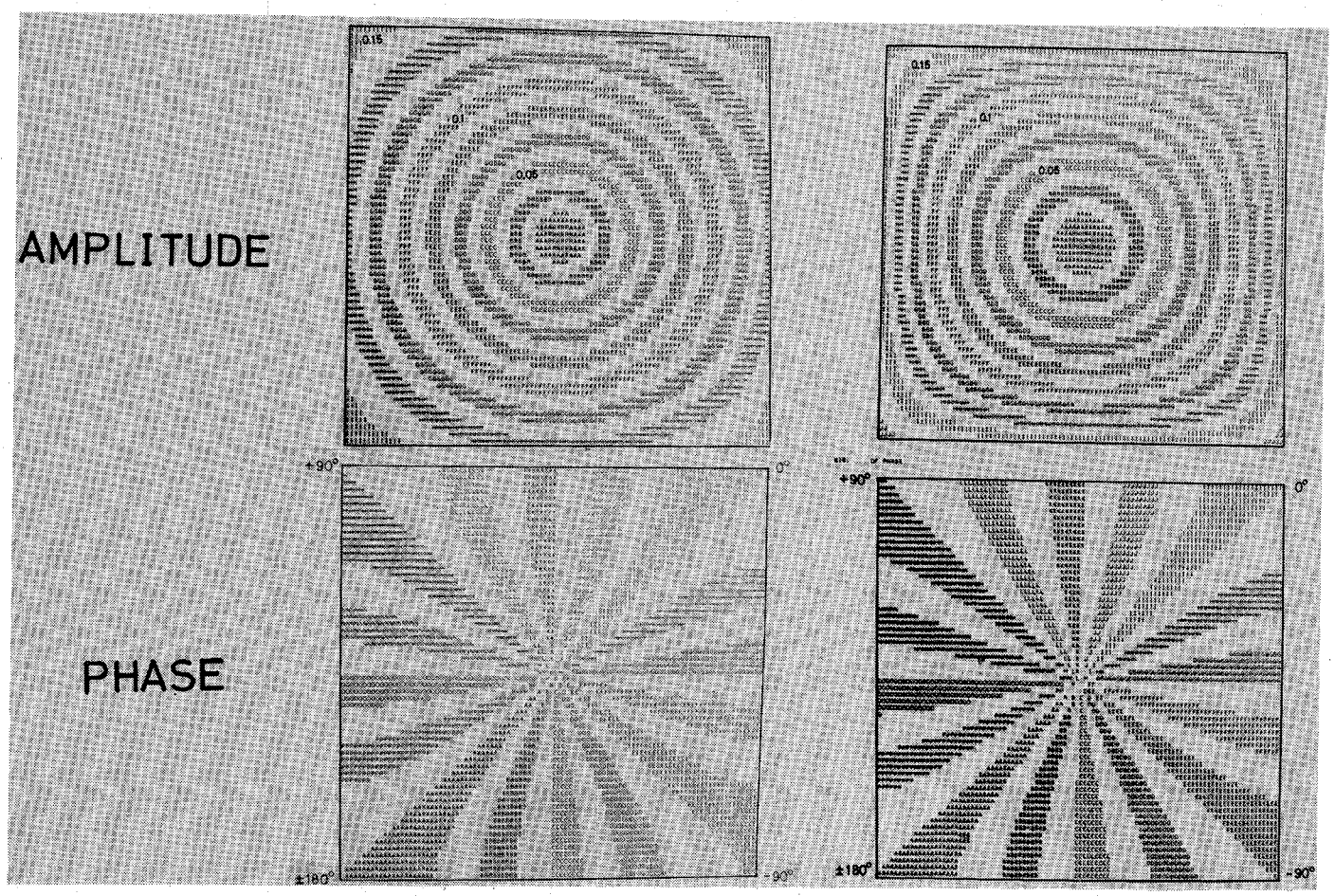

Fig. 7. Computed instantaneous distribution of the RF voltage in a square resonator for the fundamental mode. Equiamplitude (upper) and equiphase (lower) lines are shown when (a) $\mu_{eff} > 0$ at $H_0 = 1300$ Oe and (b) $\mu_{eff} < 0$ at $H_0 = 2300$ Oe.

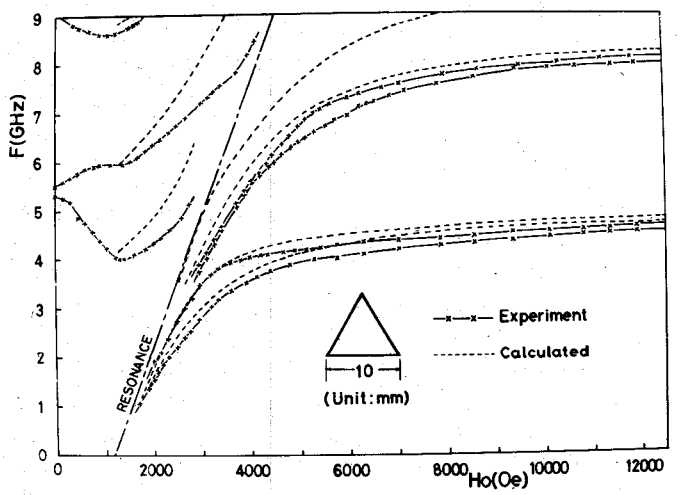

Fig. 8. Magnetic tuning characteristics of a triangular resonator.

Finally, several interesting applications of the analysis to a triangular ferrite planar circuit will be shown. Fig. 10 shows a center conductor plate of a three-port triangular circuit used in the calculation. The shaded portion (hexagon) in this figure is regarded as a planar circuit coupled by three striplines. We calculated the characteristics of the circuit for various applied magnetic fields and characteristic impedances Z_0 of the striplines. When the applied magnetic field is 5300 Oe, a circulator performance as shown in Fig. 11 was obtained above the ferrimagnetic resonance when $Z_0 = 30\ \Omega$. The light line curves are calculated by the method based upon the eigenfunction expansion for $i = a = 21$. The heavy line curves by the contour-integral method for $N = 33$ are also shown for the comparison. This performance can be explained by considering two fundamental rotating modes, i.e., a mode rotating clockwise and the other rotating counterclockwise. Consequently, the principle of operation is the same as for a disk-shaped stripline circulator.

When the applied magnetic field at the triangular ferrite planar circuit is 3300 Oe, μ_{eff} is negative in the frequency range between 7.19 and 9.24 GHz. In this range the performance of the so-called edge-guided mode circulator was calculated as shown in Fig. 12 for $Z_0 = 50\ \Omega$. We note that such a performance has not yet been obtained experimentally.

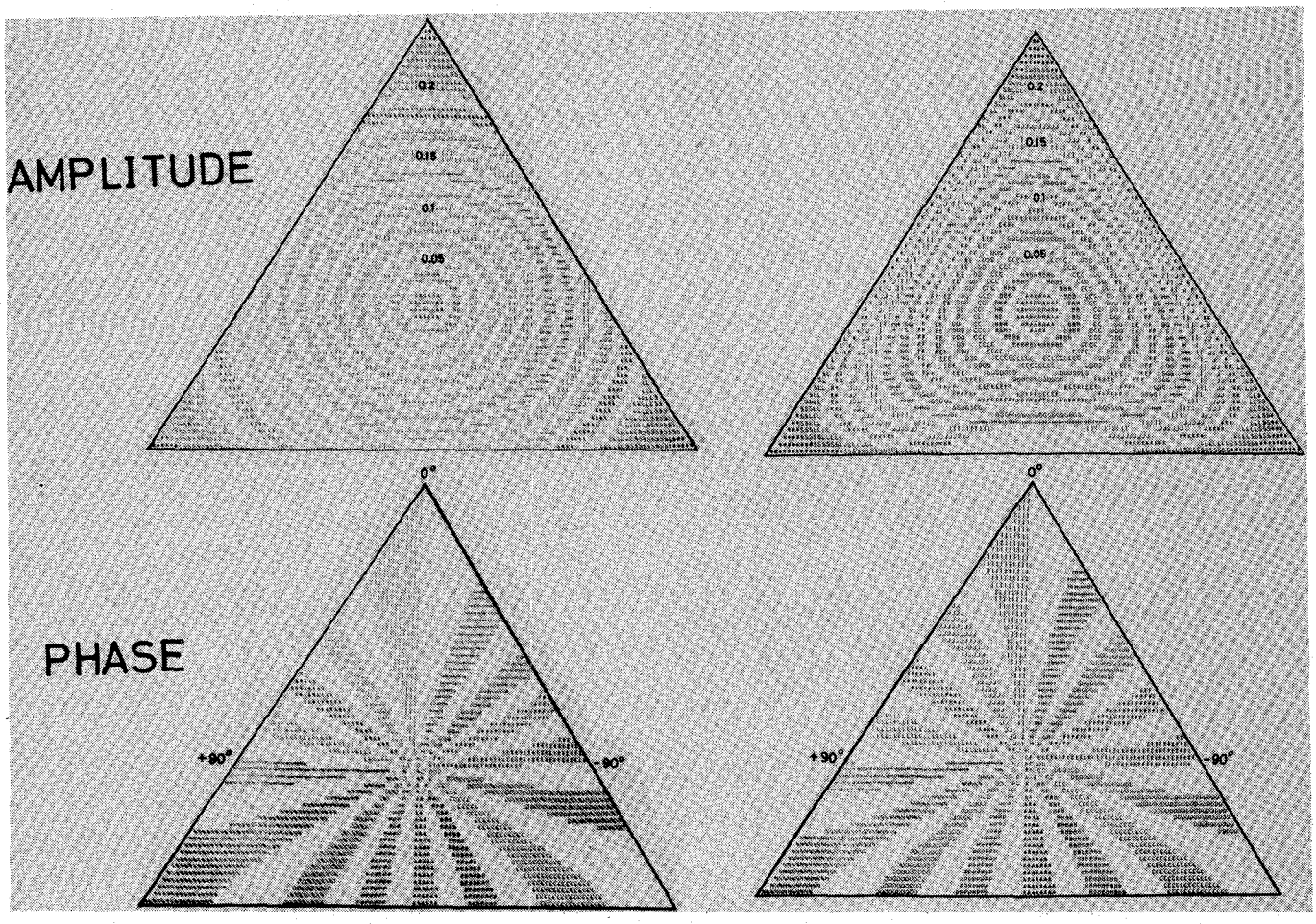

Fig. 9. Computed instantaneous distribution of the RF voltage in a triangular circuit for the fundamental mode when (a) $\mu_{eff} > 0$ at $H_0 = 1300$ Oe and (b) $\mu_{eff} < 0$ at $H_0 = 2300$ Oe.

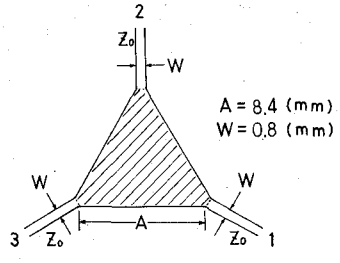

Fig. 10. Center conductor of a triangular ferrite planar circuit used in the calculation.

V. Conclusion

We have shown that an arbitrarily shaped ferrite planar circuit can be analyzed using the contour-integral method or the eigenfunction expansion method.

Although there is no difference in the labor required to analyze repeatedly at different frequencies using these two approaches, the former is more readily adapted to a circuit with a complicated pattern than the latter.

We hope that these approaches will be useful in the design and analysis of microwave integrated circuits on ferrite substrates.

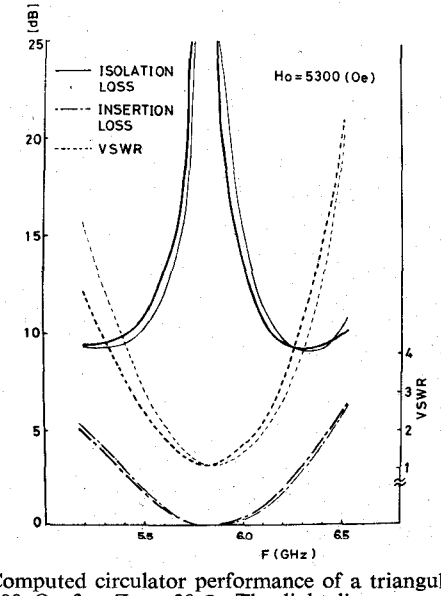

Fig. 11. Computed circulator performance of a triangular circuit at $H_0 = 5300$ Oe for $Z_0 = 30\ \Omega$. The light line curves are by the method based upon eigenfunction expansion for $i = a = 21$. The heavy line ones are by the integral equation method for $N = 33$.

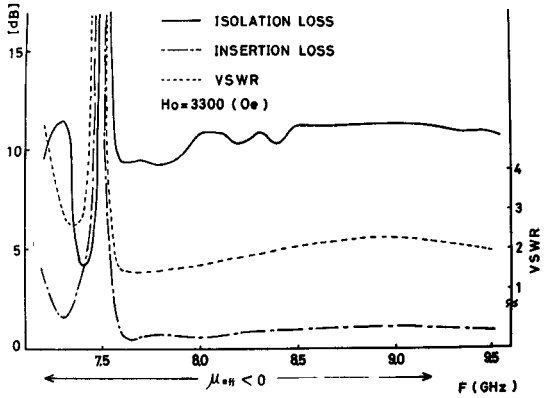

Fig. 12. Computed circulator performance of a triangular circuit at $H_0 = 3300$ Oe for $Z_0 = 50\,\Omega$.

ACKNOWLEDGMENT

The authors wish to thank Prof. T. Okoshi of University of Tokyo for his encouragement.

REFERENCES

[1] T. Okoshi, "The planar circuit," in *Rec. of Professional Groups, IECE of Japan*, Paper SSD68-37/CT68-47, Feb. 17, 1969.
[2] P. P. Civalleri and S. Ridella, "Impedance and admittance matrices of distributed three-layer *N*-ports," *IEEE Trans. Circuit Theory*, vol. CT-17, pp. 392–398, Aug. 1970.
[3] T. Okoshi and T. Miyoshi, "The planar circuit—An approach to microwave integrated circuitry," *IEEE Trans. Microwave Theory Tech.*, vol. MTT-20, pp. 245–252, Apr. 1972.
[4] P. Silvester, "Finite element analysis of planar microwave networks," *IEEE Trans. Microwave Theory Tech.*, vol. MTT-21, pp. 104–108, Feb. 1973.
[5] H. Jui-Pang, T. Anada, and O. Kondo, "Analysis of microwave planar circuits by normal mode method," *Trans. IECE of Japan*, vol. 58-B, pp. 671–678, Dec. 1974.
[6] K. Grüner, "Methods of synthesizing nonuniform waveguides," *IEEE Trans. Microwave Theory Tech.*, vol. MTT-22, pp. 317–322, Mar. 1974.
[7] F. Kato and M. Saito, "Computer-aided desigh of planar circuits," *Trans. IECE of Japan*, vol. J59-A, pp. 47–54, Jan. 1976.
[8] H. Bosma, "On stripline *Y*-circulation at UHF," *IEEE Trans. Microwave Theory Tech.*, vol. MTT-12, pp. 61–72, Jan. 1964.
[9] M. E. Hines, "Reciprocal and nonreciprocal mode of propagation in ferrite stripline and microstrip devices," *IEEE Trans. Microwave Theory Tech.*, vol. MTT-19, pp. 442–451, May 1971.
[10] P. de Santis and F. Pucci, "The edge-guided wave circulator," *IEEE Trans. Microwave Theory Tech.*, vol. MTT-23, pp. 516–519, June 1975.
[11] C. E. Fay and R. L. Comstock, "Operation of the ferrite junction circulator," *IEEE Trans. Microwave Theory Tech.*, vol. MTT-13, pp. 15–27, Jan. 1965.

Energy Analysis for the Amplification Phenomena of Magnetostatic Surface Waves in a YIG-Semiconductor Coupled System

SYOJI YAMADA, NION S. CHANG, MEMBER, IEEE, AND YUKITO MATSUO

***Abstract*—Amplification phenomena of magnetostatic surface waves (MSSW's) in a ferrite–semiconductor system are analyzed in detail for the first time from an energy view point. For the interactions between MSSW's containing a backward branch and carrier streams in a semiconductor, the dispersion relations are given and the energy conservation law is applied to the system. The results in terms of energy quantities are found to be consistent with the solutions of the dispersion equation and well explain the amplifying mechanism macroscopically. We conclude that this kind of interaction is a negative energy dissipation type of instability.**

I. INTRODUCTION

IN SEVERAL YEARS, the investigation of interaction between magnetostatic surface waves (MSSW's) and a carrier stream in semiconductor has been advanced rapidly by many authors [1]–[5]. Recently, we have proposed a general layered structure model consisting of a YIG slab, a semiconductor, dielectrics, and metal plates, and derived a general dispersion equation of the waves. As a result of the analysis, it was concluded that the MSSW's are amplified when the carrier drift velocity v_0 is greater than the phase velocity v_p of MSSW's [6], [7].

In this paper, the interaction between the MSSW mode having a backward branch [8], [9] and a stream of drifting carriers in semiconductor is discussed, including the influence of YIG damping. The ordinary dispersion equation is derived and solved numerically, and then the conservation law of energy appropriate for a dispersive medium is applied to the model of the system. The purpose of our analysis is to show the significance of the De Wames–Wolfram (WW) mode [8] in a practical amplifier design and to interpret the amplifying mechanism, which seems so far not sufficiently clear, in terms of the energy exchange between the waves and the media.

Manuscript received June 7, 1976; revised October 1, 1976.
The authors are with the Institute of Scientific and Industrial Research, Osaka University, Osaka, Japan.